A Highly Accurate Collocation Trefftz Method for Solving the Laplace Equation in the Doubly Connected Domains

Chein-Shan Liu
Department of Mechanical and Mechatronic Engineering, Taiwan Ocean University, Keelung, Taiwan

Received 9 November 2006; accepted 5 March 2007
Published online 13 June 2007 in Wiley InterScience (www.interscience.wiley.com).
DOI 10.1002/num.20257

A highly accurate new solver is developed to deal with the Dirichlet problems for the 2D Laplace equation in the doubly connected domains. We introduce two circular artificial boundaries determined uniquely by the physical problem domain, and derive a Dirichlet to Dirichlet mapping on these two circles, which are exact boundary conditions described by the first kind Fredholm integral equations. As a direct result, we obtain a modified Trefftz method equipped with two characteristic length factors, ensuring that the new solver is stable because the condition number can be greatly reduced. Then, the collocation method is used to derive a linear equations system to determine the unknown coefficients. The new method possesses several advantages: mesh-free, singularity-free, non-illposedness, semi-analyticity of solution, efficiency, accuracy, and stability. © 2007 Wiley Periodicals, Inc. Numer Methods Partial Differential Eq 24: 179–192, 2008

Keywords: artificial circles; characteristic length factors; doubly connected domain; Fredholm integral equation; Laplace equation; meshless method

I. INTRODUCTION

Numerical methods are required inevitably to solve the engineering problems governed by the partial differential equations defined in the complicated domains, since under these situations the analytical solutions are usually not available. For the solutions of engineering problems, many well-developed numerical methods such as finite difference method (FDM), finite element method (FEM), and boundary element method (BEM) are widely used. Because the BEM can reduce the dimensionality of the considered problems, it has become an efficient alternative calculational tool to replace the domain-based FDM and FEM. However, there are pitfalls to hamper its efficient implementation. The major disadvantage of BEM originates from its singularities: weak singularity of kernel function, Cauchy principal value singularity, and hypersingularity.

Correspondence to: Chein-Shan Liu, Department of Mechanical and Mechatronic Engineering, Taiwan Ocean University, Keelung, Taiwan (e-mail: csliu@mail.ntou.edu.tw)

For a complicated shape of the problem domain those standard methods usually require a large number of nodes and elements to match the geometrical shape. To overcome those difficulties, the meshless numerical methods are proposed, which are meshes free and only boundary nodes are necessary. Recently, the meshless local boundary integral equation (LBIE) method [1], and the meshless local Petrov–Galerkin (MLPG) method [2] are proposed. Both methods use local weak forms and the integrals can be easily evaluated over circles in 2D problems and spheres in 3D problems.

For problems with complicated domains, the algorithms based on the discretizations of integral equations are often attractive because of the reduced complexity of discretization when compared with the competing approach such as FEM. For this reason there were many researchers devoted to overcome the difficulties arised from the perplexing singularities in the boundary integral equations. At the first, Landweber and Macagno [3] have proposed a method to get rid of the singularity by substracting a function from the integrand so that the kernel becomes nonsingular, and then adding back an accurate integration of the function to the integral equation. This method was modified and referred to as the nonsingular boundary integral method in [4, 5], or the desingularized boundary integral method in [6].

Another way to avoid the singularity was proposed in [7–9], which move the computing nodes away from the boundary and outside the real domain of the problem. Even, this new approach can overcome the difficulties of singular integrals, it has another problem of ill-posedness due to the appearence of the first-kind Fredholm integral equations. Alternatively, Young [10] and Young et al. [11] have applied the desingularized boundary integral equation method to the potential problems. In these approaches the source points are located in the real boundary, and they regularized the singular integrals by using the Gauss' flux theorem and other property derived from the potential theory.

Our starting point is similar to the Trefftz method by using the eigenfunctions expansion. The Trefftz method satisfies the governing equation and the unknown coefficients are determined by satisfying the boundary conditions in some manners as by means of the collocation, the least square or the Galerkin method, etc. [12]. The Trefftz methods are truly meshless, since they can be implemented without either domain or surface meshing.

On the other hand, the method of fundamental solutions (MFS) [13] approximates the solution by a linear combination of fundamental solutions with singularities known as the source points located on a fictitious boundary outside the problem domain. Because the MFS is an inherently meshless boundary method and has exponential convergence property for smooth solutions, it has been used extensively for solving the Laplace equation [14]. Although the MFS can avoid the difficulties associated with the BEM, it still has the problem that the resulting linear equations system may become highly ill-conditioned when the number of source points is increased [15] or when the distances of source points are increased [16].

An improved method than the MFS is the so-called boundary knot method [17, 18] or the boundary collocation method [19, 20]. Instead of the singular fundamental solutions, these methods employed the nonsingular kernels to evaluate the homogeneous solutions. However, as pointed out by Young et al. [11] the introduction of nonsingular kernels as the radial basis functions may jeopardize the accuracy of solutions as compared with the MFS.

This paper will formulate the Laplace equation in the doubly connected domain by a modified collocation Trefftz method. Many boundary-type methods are inefficient for the non-smooth boundary curves; however, the new method is still applicable for such type boundary curves. Owing to these good properties the new method by using the modified Trefftz functions and the collocation method to determine unknown coefficients can be easily used to derive the meshless numerical method of the semi-analytical type.

II. THE PROBLEM IN DOUBLY CONNECTED DOMAIN

The problem of Laplace equation in a doubly connected domain is formulated by imposing the Dirichlet data at an exterior boundary and at an interior boundary:

$$\Delta u = u_{rr} + \frac{1}{r}u_r + \frac{1}{r^2}u_{\theta\theta} = 0, \tag{1}$$

$$u(r_3,\theta) = h_3(\theta), \quad 0 \le \theta \le 2\pi, \tag{2}$$

$$u(r_4,\theta) = h_4(\theta), \quad 0 \le \theta \le 2\pi, \tag{3}$$

where $h_3(\theta)$ and $h_4(\theta)$ are given functions, and both $r_3 = r_3(\theta)$ and $r_4 = r_4(\theta)$ are simple curves with $r_4 = r_4(\theta)$ inside $r_3 = r_3(\theta)$, i.e., $r_4(\theta) < r_3(\theta)$, $0 \le \theta < 2\pi$. Let $\Gamma_3 := \{(r,\theta)|r = r_3(\theta), 0 \le \theta < 2\pi\}$ and $\Gamma_4 := \{(r,\theta)|r = r_4(\theta),\ 0 \le \theta < 2\pi\}$. Here, we do not need to impose any smooth requirement on the boundary curves Γ_3 and Γ_4.

We replace Eqs. (2) and (3) by the following boundary conditions:

$$u(r_1,\theta) = g(\theta), \quad 0 \le \theta \le 2\pi, \tag{4}$$

$$u(r_2,\theta) = f(\theta), \quad 0 \le \theta \le 2\pi, \tag{5}$$

where both $g(\theta)$ and $f(\theta)$ are unknown functions to be determined, and $r_2 < r_1$ are constants. The requirement is that the annular with radii r_2 and r_1 can cover the entire doubly connected region, i.e., $r_2 \le r_4 < r_3 \le r_1$. The arrangement of these two artificial circles is schematically shown in Fig. 1. For this new setting, we may have a series solution

$$u(r,\theta) = \bar{a}_0 + \bar{b}_0 \ln r + \sum_{k=1}^{\infty}[(\bar{a}_k r^k + \bar{b}_k r^{-k})\cos k\theta + (\bar{c}_k r^k + \bar{d}_k r^{-k})\sin k\theta], \tag{6}$$

where the coefficients are fully determined by the boundary conditions (4) and (5) in terms of $f(\theta)$ and $g(\theta)$.

By imposing the conditions (2) and (3) on Eq. (6) we can obtain two first kind Fredholm integral equations [21]:

$$\int_0^{2\pi} K_1^3(\theta,\xi) f(\xi) d\xi - \int_0^{2\pi} K_2^3(\theta,\xi) g(\xi) d\xi = h_3(\theta), \tag{7}$$

$$\int_0^{2\pi} K_1^4(\theta,\xi) f(\xi) d\xi - \int_0^{2\pi} K_2^4(\theta,\xi) g(\xi) d\xi = h_4(\theta), \tag{8}$$

where

$$K_1^3(\theta,\xi) = \frac{\ln r_1 - \ln r_3}{2\pi(\ln r_1 - \ln r_2)} + \sum_{k=1}^{\infty} B_k^3 \cos k(\theta - \xi), \tag{9}$$

$$K_2^3(\theta,\xi) = \frac{\ln r_2 - \ln r_3}{2\pi(\ln r_1 - \ln r_2)} + \sum_{k=1}^{\infty} A_k^3 \cos k(\theta - \xi), \tag{10}$$

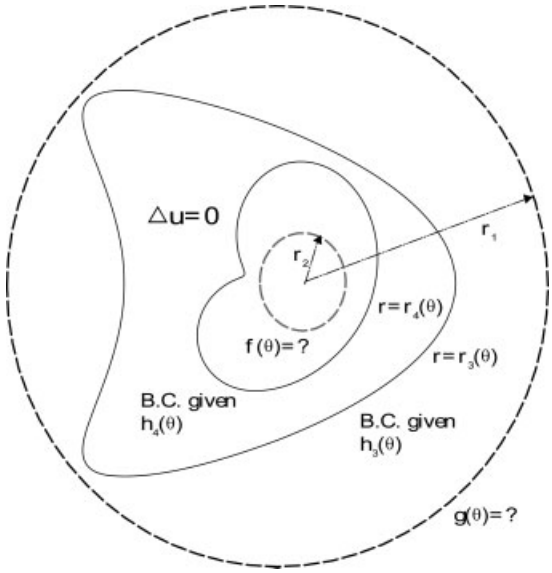

FIG. 1. Introducing two artificial circles in the plane domain, where the boundary conditions on these two circles are unknown to be determined.

$$K_1^4(\theta,\xi) = \frac{\ln r_1 - \ln r_4}{2\pi(\ln r_1 - \ln r_2)} + \sum_{k=1}^{\infty} B_k^4 \cos k(\theta - \xi), \tag{11}$$

$$K_2^4(\theta,\xi) = \frac{\ln r_2 - \ln r_4}{2\pi(\ln r_1 - \ln r_2)} + \sum_{k=1}^{\infty} A_k^4 \cos k(\theta - \xi) \tag{12}$$

are kernel functions, and

$$A_k^3 := e_k\left(r_3^{-k} r_2^k - r_3^k r_2^{-k}\right), \qquad B_k^3 := e_k\left(r_3^{-k} r_1^k - r_3^k r_1^{-k}\right), \tag{13}$$

$$A_k^4 := e_k\left(r_4^{-k} r_2^k - r_4^k r_2^{-k}\right), \qquad B_k^4 := e_k\left(r_4^{-k} r_1^k - r_4^k r_1^{-k}\right) \tag{14}$$

are all functions of θ because of $r_3 = r_3(\theta)$ and $r_4 = r_4(\theta)$. In the above e_k is defined by

$$e_k := \frac{1}{\pi\left[\left(\frac{r_1}{r_2}\right)^k - \left(\frac{r_2}{r_1}\right)^k\right]}. \tag{15}$$

III. AN EFFECTIVE COLLOCATION TREFFTZ METHOD

Equations (7) and (8) provide the Dirichlet to Dirichlet mappings on the two artificial circles. They are exact boundary conditions; however, it is difficult to directly inverse these two equations to obtain the exact boundary functions $f(\theta)$ and $g(\theta)$. Liu [21] has applied the regularization integral equation method to solve Eqs. (7) and (8), but in this paper, we are going to directly solve a variant of Eq. (6) to obtain the unknown coefficients.

For this purpose we let

$$a_0 = \bar{a}_0, \qquad a_k = \bar{a}_k r_1^k, \qquad b_k = \bar{b}_k r_2^{-k}, \tag{16}$$

$$b_0 = \bar{b}_0, \qquad c_k = \bar{c}_k r_1^k, \qquad d_k = \bar{d}_k r_2^{-k}, \tag{17}$$

and thus Eq. (6) can be expressed as

$$u(r,\theta) = a_0 + b_0 \ln r + \sum_{k=1}^{\infty} \left[\left(a_k \left(\frac{r}{r_1} \right)^k + b_k \left(\frac{r_2}{r} \right)^k \right) \cos k\theta + \left(c_k \left(\frac{r}{r_1} \right)^k + d_k \left(\frac{r_2}{r} \right)^k \right) \sin k\theta \right], \tag{18}$$

where

$$r_1 \geq \max_{\theta \in [0,2\pi]} r_3(\theta), \tag{19}$$

$$r_2 \leq \min_{\theta \in [0,2\pi]} r_4(\theta). \tag{20}$$

Usually, one may take $r_1 = \max r_3(\theta)$ and $r_2 = \min r_4(\theta)$.

The numerical examples given in the next section will explain why the new method is workable. The series expansion in Eq. (18) is well suited to the entire solution domain. Hence, the following admissible functions with finite terms can be used:

$$u(r,\theta) = a_0 + b_0 \ln r + \sum_{k=1}^{m} \left[A_k^r a_k + B_k^r b_k + C_k^r c_k + D_k^r d_k \right], \tag{21}$$

where

$$A_k^r = \left(\frac{r}{r_1} \right)^k \cos k\theta, \tag{22}$$

$$B_k^r = \left(\frac{r_2}{r} \right)^k \cos k\theta, \tag{23}$$

$$C_k^r = \left(\frac{r}{r_1} \right)^k \sin k\theta, \tag{24}$$

$$D_k^r = \left(\frac{r_2}{r} \right)^k \sin k\theta. \tag{25}$$

In Eq. (21) there are totally $4m + 2$ unknown coefficients. Equation (21) is imposed at different collocated points on two different boundaries with $[r_3(\theta_i), \theta_i] \in \Gamma_3$ and $[r_4(\theta_i), \theta_i] \in \Gamma_4$ to pointwisely match the boundary conditions (2) and (3):

$$a_0 + b_0 \ln r_3(\theta_i) + \sum_{k=1}^{m} \left[A_k^{r_3}(\theta_i) a_k + B_k^{r_3}(\theta_i) b_k + C_k^{r_3}(\theta_i) c_k + D_k^{r_3}(\theta_i) d_k \right] = h_3(\theta_i), \tag{26}$$

$$a_0 + b_0 \ln r_4(\theta_i) + \sum_{k=1}^{m} \left[A_k^{r_4}(\theta_i) a_k + B_k^{r_4}(\theta_i) b_k + C_k^{r_4}(\theta_i) c_k + D_k^{r_4}(\theta_i) d_k \right] = h_4(\theta_i). \tag{27}$$

When the index i in Eqs. (26) and (27) runs from 1 to $2m+1$ we obtain a linear equations system with dimensions $n = 4m + 2$:

$$\begin{bmatrix} 1 & \ln r_3(\theta_1) & A_1^{r_3}(\theta_1) & B_1^{r_3}(\theta_1) & C_1^{r_3}(\theta_1) & D_1^{r_3}(\theta_1) & \dots \\ 1 & \ln r_4(\theta_1) & A_1^{r_4}(\theta_1) & B_1^{r_4}(\theta_1) & C_1^{r_4}(\theta_1) & D_1^{r_4}(\theta_1) & \dots \\ \vdots & \vdots & \vdots & \vdots & \vdots & \vdots & \vdots \\ 1 & \ln r_3(\theta_{2m+1}) & A_1^{r_3}(\theta_{2m+1}) & B_1^{r_3}(\theta_{2m+1}) & C_1^{r_3}(\theta_{2m+1}) & D_1^{r_3}(\theta_{2m+1}) & \dots \\ 1 & \ln r_4(\theta_{2m+1}) & A_1^{r_4}(\theta_{2m+1}) & B_1^{r_4}(\theta_{2m+1}) & C_1^{r_4}(\theta_{2m+1}) & D_1^{r_4}(\theta_{2m+1}) & \dots \end{bmatrix}$$

$$\begin{bmatrix} A_m^{r_3}(\theta_1) & B_m^{r_3}(\theta_1) & C_m^{r_3}(\theta_1) & D_m^{r_3}(\theta_1) \\ A_m^{r_4}(\theta_1) & B_m^{r_4}(\theta_1) & C_m^{r_4}(\theta_1) & D_m^{r_4}(\theta_1) \\ \vdots & \vdots & \vdots & \vdots \\ A_m^{r_3}(\theta_{2m+1}) & B_m^{r_3}(\theta_{2m+1}) & C_m^{r_3}(\theta_{2m+1}) & D_m^{r_3}(\theta_{2m+1}) \\ A_m^{r_4}(\theta_{2m+1}) & B_m^{r_4}(\theta_{2m+1}) & C_m^{r_4}(\theta_{2m+1}) & D_m^{r_4}(\theta_{2m+1}) \end{bmatrix} \begin{bmatrix} a_0 \\ b_0 \\ a_1 \\ b_1 \\ c_1 \\ d_1 \\ \vdots \\ a_m \\ b_m \\ c_m \\ d_m \end{bmatrix} = \begin{bmatrix} h_3(\theta_1) \\ h_4(\theta_1) \\ \vdots \\ h_3(\theta_{2m+1}) \\ h_4(\theta_{2m+1}) \end{bmatrix}. \quad (28)$$

We denote the above equation by

$$\mathbf{Re} = \mathbf{b}_1,$$

where $\mathbf{e} = [a_0, b_0, a_1, b_1, c_1, d_1, \dots, a_m, b_m, c_m, d_m]^{\mathrm{T}}$ is the vector of unknown coefficients. The conjugate gradient method can be used to solve the following normal equation:

$$\mathbf{Ae} = \mathbf{b}, \quad (29)$$

where

$$\mathbf{A} := \mathbf{R}^{\mathrm{T}}\mathbf{R}, \qquad \mathbf{b} := \mathbf{R}^{\mathrm{T}}\mathbf{b}_1. \quad (30)$$

Inserting the calculated $\mathbf{e}$ into Eq. (21) we thus have a semi-analytical solution of $u(r, \theta)$:

$$u(r,\theta) = e_1 + e_2 \ln r + \sum_{k=1}^{m} \left[\left(e_{4k-1} \left(\frac{r}{r_1} \right)^k + e_{4k} \left(\frac{r_2}{r} \right)^k \right) \cos k\theta + \left(e_{4k+1} \left(\frac{r}{r_1} \right)^k + e_{4k+2} \left(\frac{r_2}{r} \right)^k \right) \sin k\theta \right], \quad (31)$$

where $(e_1, \dots, e_n)$ are the components of $\mathbf{e}$.

IV. NUMERICAL TESTS AND COMMENTS ON THE NEW METHOD

A. Example 1

We consider a kite-shape outer boundary with the parameterization given by

$$r_3 = \sqrt{(0.6\cos\theta + 0.3\cos 2\theta - 0.2)^2 + (0.6\sin\theta)^2}, \quad (32)$$

$$x_3(\theta) = r_3 \cos\theta, \qquad y_3(\theta) = r_3 \sin\theta. \tag{33}$$

For the inner boundary we consider an apple shape described by

$$r_4 = \frac{0.5 + 0.2\cos\theta + 0.1\sin 2\theta}{1.5 + 0.7\cos\theta}, \tag{34}$$

$$x_4(\theta) = r_4 \cos\theta, \qquad y_4(\theta) = r_4 \sin\theta. \tag{35}$$

The above two curves are shown in the inset of Fig. 2.

To test our method we consider an exact solution

$$u(r,\theta) = x^2 - y^2 = r^2 \cos 2\theta, \tag{36}$$

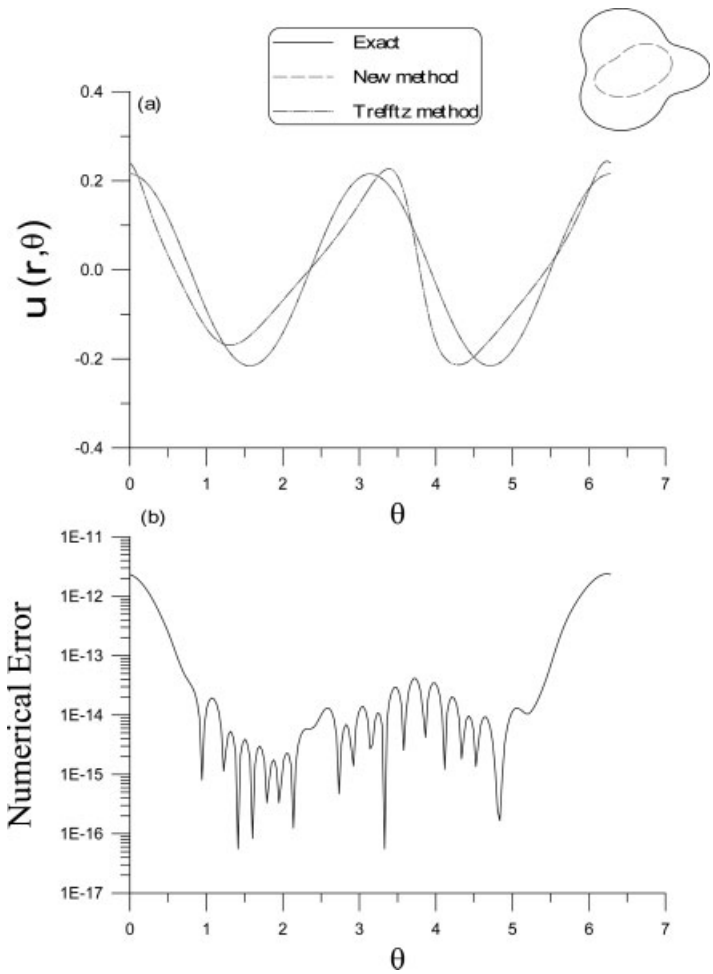

FIG. 2. For Example 1: (a) comparing the numerical and exact solutions, and (b) plotting the numerical error.

which however led to very complicated boundary conditions given as follows:

$$h_3(\theta) = u(r_3, \theta) = [(0.6\cos\theta + 0.3\cos 2\theta - 0.2)^2 + (0.6\sin\theta)^2]\cos 2\theta, \tag{37}$$

$$h_4(\theta) = u(r_4, \theta) = \left(\frac{0.5 + 0.2\cos\theta + 0.1\sin 2\theta}{1.5 + 0.7\cos\theta}\right)^2 \cos 2\theta. \tag{38}$$

Under the parameters $r_1 = \max r_3$, $r_2 = \min r_4$, and $m = 15$, we solve this problem by the method in Section III, whose result along a circle with the radius $r = \max r_4$ is shown in Fig. 2(a). Through 546 iterations the solution of $\mathbf{e}$ by Eq. (29) is obtained under a stopping criterion 10^{-15}. The numerical error of u is shown in Fig. 2(b), which can be seen is smaller than 3×10^{-12}. A highly accurate result is obtained as compared with the exact solution.

When we apply the Trefftz method on this problem by using $r_1 = 1$, $r_2 = 1$, and $m = 15$, we find that the solution is unstable as shown in Fig. 2(a) by the dashed-dotted line.

All the computations in this paper are carried out in a PC-586 with pentium-100. For this example, the computations both by the Trefftz method and our new method spent the CPU time smaller than one second. Basically, the most time is spent in the solution of Eq. (29). Under the same stopping criterion, through 467 iterations the solution of $\mathbf{e}$ by Eq. (29) is obtained for the Trefftz method. Because of the small difference of the numbers of iterations of these two methods, the computational times are almost the same. Indeed, the new method does not require any extra effort to prepare a new program; both two methods can use the same program, but with different input parameters of r_1 and r_2 fed in the program.

To observe the stable phenomenon of the new method and the unstable behavior of the Trefftz method we plot the condition number of $\mathbf{A}$ with different number of bases in Fig. 3, which is defined by

$$\text{Cond}(\mathbf{A}) = \|\mathbf{A}\|\|\mathbf{A}^{-1}\|. \tag{39}$$

The norm used for $\mathbf{A}$ is the Frobenius norm. Therefore, we have

$$\frac{1}{n}\text{Cond}(\mathbf{A}) \le \frac{\lambda_{\max}(\mathbf{A})}{\lambda_{\min}(\mathbf{A})} \le \text{Cond}(\mathbf{A}), \tag{40}$$

where λ is the eigenvalue of $\mathbf{A}$. Conventionally, $\lambda_{\max}(\mathbf{A})/\lambda_{\min}(\mathbf{A})$ is used to define the condition number of $\mathbf{A}$. For the present study we use Eq. (39) to define the condition number of $\mathbf{A}$.

As mentioned by Kita et al. [12] when one uses the Trefftz boundary type method, the condition number may increase fast as the number of elements increases. It can be seen that the present method can greatly reduce the condition number. Therefore, when the new method is very accurate, the Trefftz method leads to a bad numerical result as shown in Fig. 2(a).

B. Comments on the New Method

After showing the effect of the new method through a numerical example and comparing the condition numbers for the new method and the Trefftz method, it is now a good position to give some comments on the new method.

It is known that for the Laplace equation in the two-dimensional doubly connected domain the set

$$\{1, \ln r, r^{\pm k}\cos k\theta, r^{\pm k}\sin k\theta,\ k = 1, 2, \ldots\} \tag{41}$$

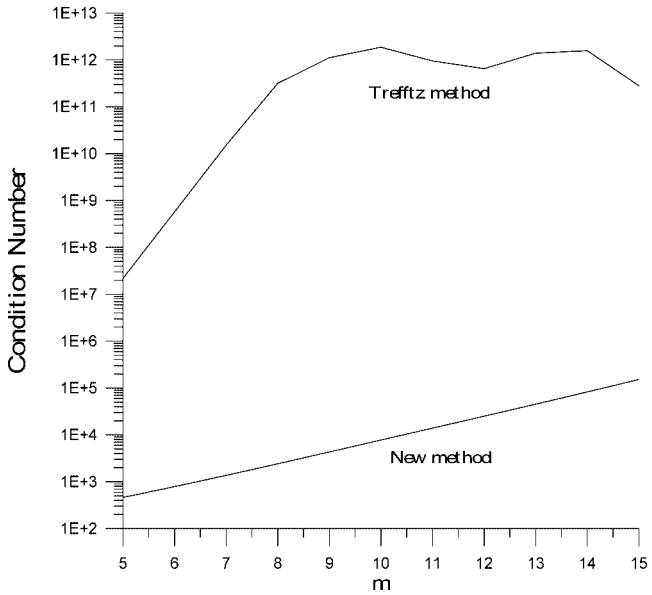

FIG. 3. For Example 1 we comparing the condition number with respect to m for the Trefftz method and the new method.

forms the T-complete functions, and the solution can be expanded by these bases [12, 22]:

$$u(r,\theta) = a_0 + b_0 \ln r + \sum_{k=1}^{\infty} [(a_k r^k + b_k r^{-k}) \cos k\theta + (c_k r^k + d_k r^{-k}) \sin k\theta]. \tag{42}$$

This method is named the Trefftz method. It can be seen that the new method is an extension of the Trefftz method. Inserting $r_1 = r_2 = 1$ into Eq. (18), we can recover to the Trefftz method.

Our starting point in Eq. (18) is similar to the Trefftz method. However, the present modification is suggested to use a new set of T-complete bases by

$$\left\{1, \ln r, \left(\frac{r}{r_1}\right)^k \cos k\theta, \left(\frac{r}{r_1}\right)^k \sin k\theta, \left(\frac{r_2}{r}\right)^k \cos k\theta, \left(\frac{r_2}{r}\right)^k \sin k\theta,\ k = 1, 2, \ldots\right\}. \tag{43}$$

The above set is a very natural result from the concept of the artificial circles with radii r_1 and r_2, where two exact boundary conditions can be established by solving Eqs. (7) and (8). The factors of r_1 and r_2 indeed play a major role to stabilize the conventional Trefftz method.

For the Trefftz method the numerical instability is an inherent property, which uses the power functions r^k and $(1/r)^k$ in the bases, a main reason to cause the numerical instability, because r may be greater than 1 or may be smaller than 1. When the problem domain has a larger size with its largest length of the boundary points to the origin being greater than 1, the powers r^k are divergent, and similarly, when the problem domain has a smaller size with its smallest length of

the boundary points to the origin being smaller than 1, the powers $(1/r)^k$ are divergent. They are thus inevitably led to the numerical instability.

But in our modification the situation is drastically different. For the doubly connected problem its domain is $r_4 < r < r_3$. Thus the power functions $(r/r_1)^k$ in Eq. (43) are always smaller than 1 because of Eq. (19), and similarly, the power functions $(r_2/r)^k$ in Eq. (43) are always smaller than 1 because of Eq. (20).

It has been clear that the factors of characteristic lengths r_1 and r_2 ensure the stability of the modified Trefftz method. Through this new modification the condition number of the linear equations system can be greatly reduced as already shown in Fig. 3 for Example 1. For the following other examples this is also true.

To our best knowledge, the new concept does not appear in the literatue of the Trefftz method; see, e.g., Kita and Kamiya [12] and Li et al. [22].

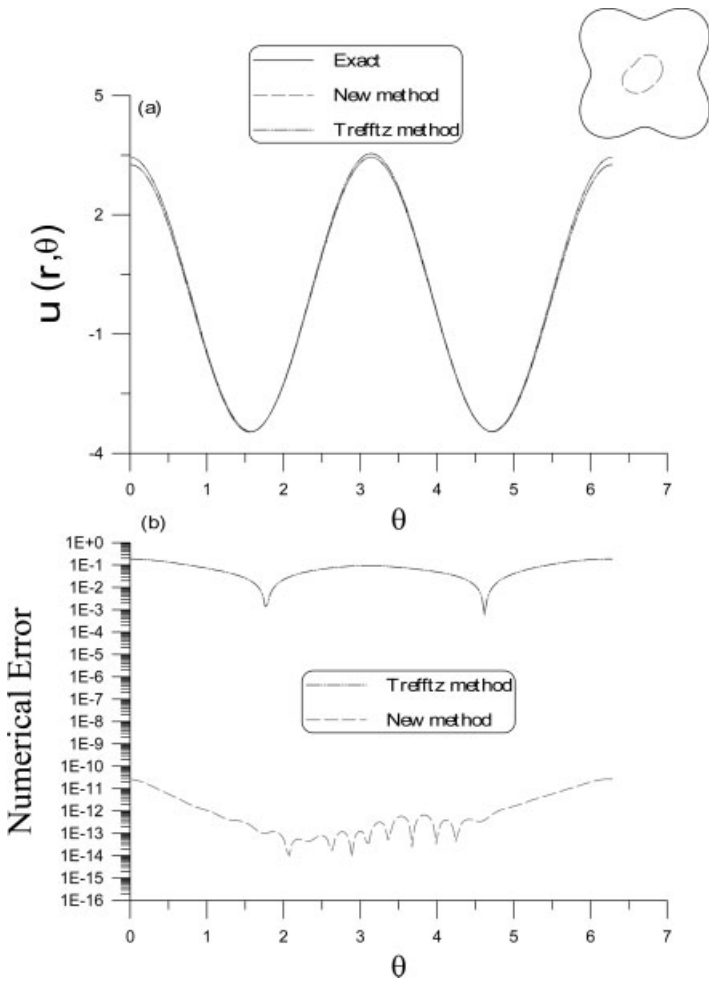

FIG. 4. For Example 2: (a) comparing the exact solution and the numerical ones of Trefftz method and new method, and (b) plotting the numerical errors.

C. Example 2

Next we replace the outer boundary by a complex epitrochoid boundary shape

$$r_3(\theta) = \sqrt{(a+b)^2 + 1 - 2(a+b)\cos(a\theta/b)}, \tag{44}$$

$$x_3(\theta) = r_3 \cos\theta, \qquad y_3(\theta) = r_3 \sin\theta \tag{45}$$

with $a = 4$ and $b = 1$. The inner boundary is four times large of the above kite. The above two curves are shown in the inset of Fig. 4.

Under the parameters $r_1 = \max r_3$, $r_2 = \min r_4$, and $m = 13$, we solve this problem by the method in Section III, whose result along a circle with the radius $r = \max r_4$ is shown in Fig. 4(a) by the dashed line. The numerical error of u is shown in Fig. 4(b), which can be seen is smaller than 5×10^{-11}. A highly accurate result is obtained as compared with the exact solution $u(x, y) = x^2 - y^2$. However, when we apply the Trefftz method on this case under the parameters $r_1 = 1$, $r_2 = 1$ and $m = 13$, the solution as shown in Fig. 4(a) by the dashed-dotted line slightly deviates from the exact solution. It is not accurate when comparing with the new method. The

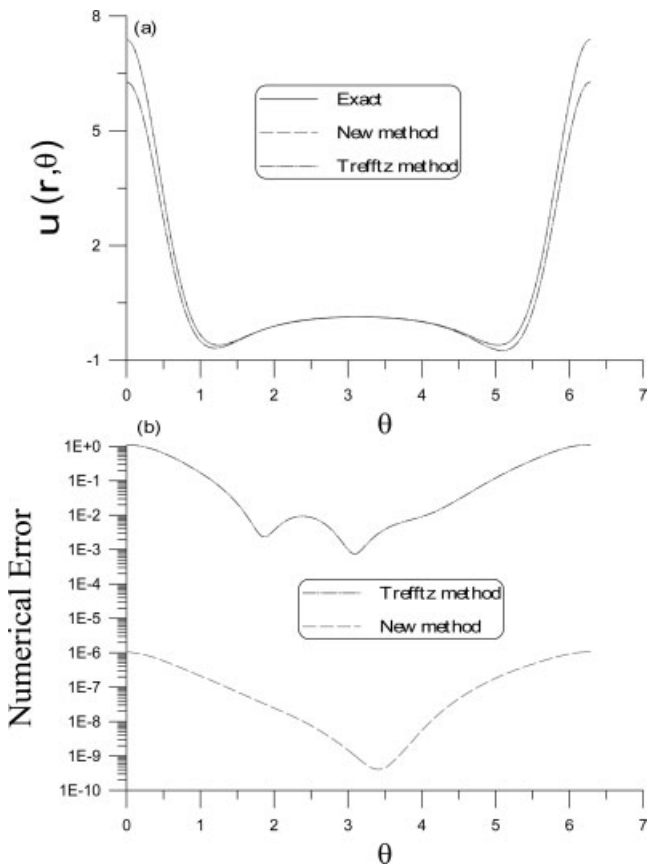

FIG. 5. For Example 3: (a) comparing the exact solution and the numerical ones of Trefftz method and new method, and (b) plotting the numerical errors.

present method can largely improve the accuracy about ten orders than the Trefftz method when it is applicable. For this example both two methods spent the CPU time smaller than one second.

D. Example 3

We consider the same boundaries as that used in the previous example but with the following closed form solution

$$u(r,\theta) = e^x \cos y = e^{r\cos\theta}\cos(r\sin\theta). \tag{46}$$

The boundary conditions are very complicated for this example.

Under the parameters $r_1 = \max r_3$, $r_2 = \min r_4$, and $m = 20$, we solve this problem by the method in Section III, whose result along a circle with the radius $r = 2$ is shown in Fig. 5(a) by the dashed line. The numerical error of u is shown in Fig. 5(b), which can be seen is smaller than

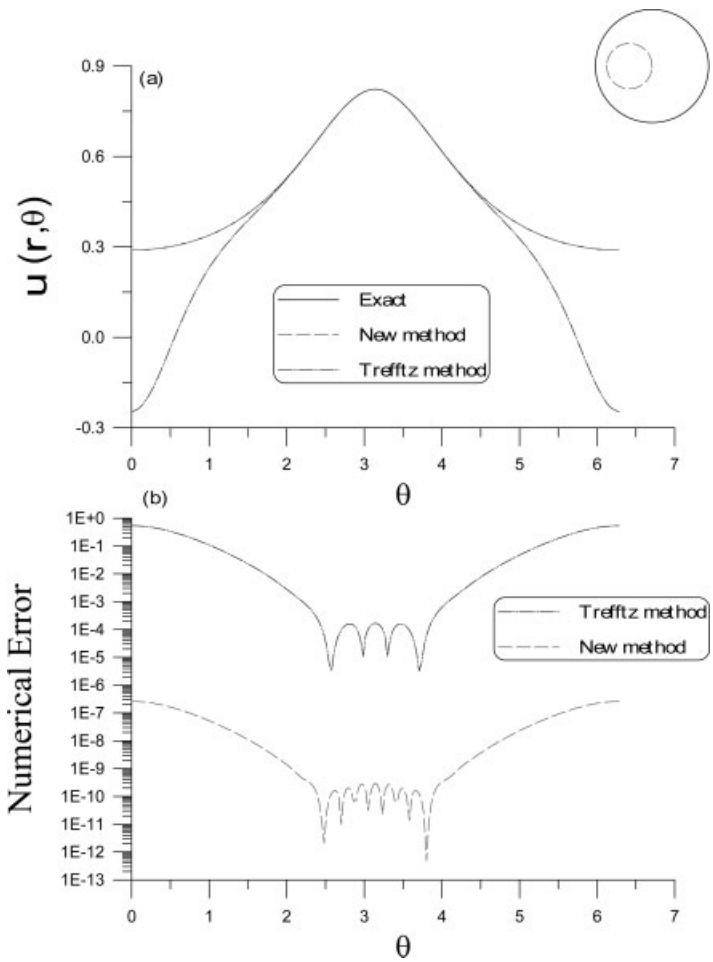

FIG. 6. For Example 4: (a) comparing the exact solution and the numerical ones of Trefftz method and new method, and (b) plotting the numerical errors.

10^{-6}. However, when we apply the Trefftz method on this example under the parameters $r_1 = 1$, $r_2 = 1$ and $m = 10$, the solution as shown in Fig. 5(a) by the dashed-dotted line slightly deviates from the exact solution. The numerical error of u is very large in the order of 1. For this example both two methods spent the CPU time smaller than one second.

E. Example 4

In this example we consider the Laplace equation in an eccentric annular domain as shown in the inset of Fig. 6, where the inner boundary is simply a unit circle with $r_4 = 1$, and the outer boundary is described by

$$r_3(\theta) = \cos\theta + \sqrt{\cos^2\theta + 21/4}. \tag{47}$$

Under the boundary conditions

$$u(r_4, \theta) = 0, \qquad u(r_3, \theta) = 1, \tag{48}$$

we have a closed-form solution

$$u(r, \theta) = \frac{1}{\ln 4} \ln\left(\frac{16r^2 + 1 + 8r\cos\theta}{r^2 + 16 + 8r\cos\theta}\right). \tag{49}$$

Under the parameters $r_1 = 4$, $r_2 = 0.8$ and $m = 20$, we solve this problem by the method in Section III, whose result along a circle with the radius $r = 1.4$ is shown in Fig. 6(a) by the dashed line, while the exact solution calculated from Eq. (49) is represented by the solid line. The numerical error of u is shown in Fig. 6(b), which can be seen is smaller than 5×10^{-7}. When we apply the Trefftz method on this case under the parameters $r_1 = 1$, $r_2 = 1$ and $m = 11$ ($m = 20$ cannot be applicable), the solution as shown in Fig. 6(a) by the dashed-dotted line largely deviates from the exact solution. For this example both two methods spent the CPU time smaller than one second.

V. CONCLUSIONS

In this paper we have proposed a new meshless method to calculate the solutions of Laplace equation in the arbitrary doubly connected plane domains. To tackle of the ill-conditioning of the Trefftz method, we have employed two characteristic length factors into the basis functions. This type formulation is a very natural result in terms of the concept of artificial circles. The numerical examples show that the present method is highly accurate; for example, for the first two examples the accuracy can be achieved is up to 10^{-11} of the absolute error. The new method possesses several advantages, including mesh-free, singularity-free, non-illposedness, accuracy and stability, deserved its extension to other elliptic type boundary-value problems.

References

1. S. N. Atluri, H. G. Kim, and J. Y. Cho, A critical assessment of the truly meshless local Petrov–Galerkin (MLPG), and local boundary integral equation (LBIE) methods, Comput Mech 24 (1999), 348–372.
2. S. N. Atluri and S. Shen, The meshless local Petrov–Galerkin (MLPG) method: a simple & less-costly alternative to the finite element and boundary element methods, Comput Model Eng Sci 3 (2002), 11–51.

3. L. Landweber and M. Macagno, Irrotational flow about ship forms, IIHR Report No. 123, Iowa University, 1969.
4. W. S. Hwang and Y. Y. Huang, Nonsingular direct formulation of boundary integral equations for potential flows, Int J Numer Methods Fluids 26 (1998), 627–635.
5. C. M. Fan and D. L. Young, Analysis of the 2D Stokes flows by the nonsingular boundary integral equation method, Int Math J 2 (2002), 1199–1215.
6. J. M. Chuang, Numerical studies on desingularized Cauchy's formula with applications to interior potential problems, Int J Numer Methods Eng 46 (1999), 805–824.
7. Y. Cao, W. W. Schultz, and R. F. Beck, Three-dimensional desingularized boundary integral methods for potential problems, Int J Numer Methods Fluids 12 (1991), 785–803.
8. F. Lalli, On the accuracy of the desingularized boundary integral method in free surface flow problems, Int J Numer Methods Fluids 25 (1991), 1163–1184.
9. Y. L. Zhang, K. S. Yeo, B. C. Khoo, and W. K. Chong, Simulation of three-dimensional bubbles using desingularized boundary integral method, Int J Numer Methods Fluids 31 (1999), 1311–1320.
10. S. A. Young, A solution method for two-dimensional potential flow about bodies with smooth surfaces by direct use of the boundary integral equation, Commun Numer Methods Eng 15 (1999), 469–478.
11. D. L. Young, K. H. Chen, and C. W. Lee, Novel meshless method for solving the potential problems with arbitrary domain, J Comput Phys 209 (2005), 290–321.
12. E. Kita and N. Kamiya, Trefftz method: an overview, Adv Eng Softw 24 (1995), 3–12.
13. G. Fairweather and A. Karageorghis, The method of fundamental solutions for elliptic boundary value problems, Adv Comput Math 9 (1998), 69–95.
14. I. Saavedra and H. Power, Multipole fast algorithm for the least-squares approach of the method of fundamental solutions for three-dimensional harmonic problems, Numer Methods Partial Differential Equations 19 (2003), 828–845.
15. M. A. Golberg and C. S. Chen, Discrete projection methods for integral equations, Computational Mechanics Publications, Southampton, 1996.
16. C. S. Chen, H. A. Cho, and M. A. Golberg, Some comments on the ill-conditioning of the method of fundamental solutions, Eng Anal Boundary Elem 30 (2006), 405–410.
17. W. Chen and M. Tanaka, A meshless, integration-free, and boundary-only RBF technique, Comput Math Appl 43 (2002), 379–391.
18. B. Jin and W. Chen, Boundary knot method based on geodesic distance for anisotropic problems, J Comput Phys 215 (2006), 614–629.
19. J. T. Chen, M. H. Chang, K. H. Chen, and S. R. Lin, The boundary collocation method with meshless concept for acoustic eigenanalysis of two-dimensional cavities using radial basis function, J Sound Vibration 257 (2002), 667–711.
20. J. T. Chen, M. H. Chang, K. H. Chen, and I. L. Chen, Boundary collocation method for acoustic eigenanalysis of three-dimensional cavities using radial basis function, Comput Mech 29 (2002), 392–408.
21. C. S. Liu, A meshless regularized integral equations method (MRIEM) for solving the Laplace equation in the doubly connected domain, Proceeding of the 2nd Asia-Pacific International Conference on Computational Methods in Engineering, Nov. 14–16, 2006.
22. Z. C. Li, T. T. Lu, H. T. Huang, and A. H. D. Cheng, Trefftz, collocation, and other boundary methods—a comparison, Numer Methods Partial Differential Equations 23 (2006), 93–144.